A coupled mechanistic and reservoir-computing model of a stirred-yoghurt line built from public data

Heat treatment, fermentation, texture, energy and equipment sizing, with a case study in Akbou (Algeria)

A.Benahmed
Conservatoire National des Arts et Métiers (CNAM), France
abenahmed1@gmail.com

Abstract

This paper couples four standard models of a stirred-yoghurt line (denaturation of β-lactoglobulin during heat treatment, growth and acidification by the starter, texture and syneresis of the stirred gel, specific energy of the line) and uses the result to pick an operating point and size the main equipment. An echo state network corrects the residual between model and plant pH. All parameters come from the literature. The plant context is a large dairy site in Akbou, Algeria, known to me only through public sources: I had no access to company data, and the signals used to train the correction are synthetic. Under these assumptions the batch reaches pH 4.6 in 4.09 h at 42 °C. The optimizer drives the heat treatment to 95 °C and 600 s and the smoothing shear down to 60 s^{-1}, which lowers predicted syneresis from 12.4% to 8.7% and specific energy by 1.8%. Every starting point ends in this corner, mostly because fouling, cooked flavour and the cost of the holding tube are missing from the objective. The texture and syneresis laws have not been fitted to measurements. I state which parts of the model are established and which are assumed, and give a calibration protocol; the notebook and scripts are attached.

1 Introduction

Stirred yoghurt is made in a short chain of operations whose effects are tightly coupled. The heat treatment of the milk, typically 85–95 °C for a few minutes, denatures most of the whey protein β-lactoglobulin, which then associates with the casein micelles and strengthens the acid gel formed later. Fermentation by *Streptococcus thermophilus* and *Lactobacillus delbrueckii* subsp. *bulgaricus* lowers the pH to about 4.6, the isoelectric point of the caseins. The gel is then broken, smoothed and pumped, and its final viscosity and its tendency to expel whey depend on all three previous steps. Most of the energy goes into heating and cooling the milk.

Taken one by one, these steps have well-known models: reaction kinetics for the denaturation of whey proteins [1], cardinal-temperature growth models [2], the Luedeking–Piret law for product formation [3] and the Herschel–Bulkley law for the flow of yoghurt [4]. Putting them in one model lets a change in the heat treatment be followed through to texture, energy and the size of tanks and pipes; this mechanistic core is roughly what people mean by a digital twin of a line. Since no such model is exact, a data-driven term trained on plant signals is often added on top. I used reservoir computing [5] for that term because its training is a linear regression.

The case study is the site of Laiterie Soummam in Akbou (Béjaïa, Algeria). It lends itself to the exercise because press reports and the company's own statements give enough figures to bound the main assumptions (Section 2). I have no link with the company and used none of its data; the line modelled here is a generic line placed in the context of that site. Two further limits matter when reading the results. The plant signals used to train the correction are synthetic, so Section 5.2 shows that the method can learn a known drift and tells us nothing about a real

residual. And the coefficients of the texture and syneresis laws were set by hand to give plausible values; none of them was fitted. Section 6 lists the measurements that would turn the model into a description of an actual line.

2 Public context of the case study

Table 1 collects the public information used to bound the assumptions. The company reports a production of about 2 000 t of dairy products per day in 2023, and claimed 8 million pots of yoghurt per day as early as 2013 [14]. Raw milk collection was reported at about 700 000 L per day and 250 million litres in 2024 [15]; other statements give figures between 400 000 and 860 000 L per day depending on the period [16, 17]. In 2024 fresh milk reportedly accounted for 40–50% of the milk used in the company's products [16], and the label of a 90 g flavoured stirred yoghurt lists whole milk and reconstituted whole milk [19]. The share of reconstituted milk is therefore a plausible source of batch-to-batch variability, together with the seasonal variation of collection. The two production units are in the Taharacht industrial zone of Akbou [18], at an elevation of about 273 m, with an annual mean temperature of about 17.6 °C and a mean July maximum of about 34 °C [20].

Table 1: Public information on the site used to bound the model assumptions.

Item	Reported value	Source
Location	two units, Taharacht industrial zone, Akbou	[18]
Production (2023)	≈ 2 000 t/day, all dairy products	[14]
Yoghurt	8 million pots/day claimed in 2013	[14]
Raw milk collection	≈ 700 000 L/day, 250 million L in 2024; other reports 400 000–860 000 L/day	[15, 16, 17]
Fresh milk share (2024)	40–50%	[16]
Stirred yoghurt recipe	whole milk, reconstituted whole milk, sugar; 90 g pot	[19]
Climate	annual mean ≈ 17.6 °C, July mean maximum ≈ 34 °C	[20]

I use these figures for two checks only. The milk composition assumed in the model (Section 3) is checked to be of the right order, and the throughput of one modelled line is compared with the claimed yoghurt volume: 8 million pots of 90–100 g correspond to 720–800 t/day, that is 3.3 to 3.7 lines of 2.5 kg s^{-1} running continuously. The share of stirred yoghurt in that volume and the actual number of lines are not public.

3 Model

Figure 1 shows the structure of the model. The milk is treated as a homogeneous, perfectly mixed volume at each stage (a zero-dimensional model). The operating variables are $\mathbf{x} = (T_{\mathrm{past}}, t_{\mathrm{hold}}, T_{\mathrm{ferm}}, \dot{\gamma}_{\mathrm{pump}})$: heat-treatment temperature, holding time, fermentation temperature and the shear rate applied when the gel is smoothed and pumped. SI units are used throughout; temperatures are in kelvin in the equations and in degrees Celsius in the text when that is clearer.

3.1 Heat treatment

The native β-lactoglobulin concentration C_β decreases with an apparent reaction order of 1.5, the order reported by Dannenberg and Kessler for milk [1]:

$$\frac{\mathrm{d}C_\beta}{\mathrm{d}t} = -k_d(T)\, C_\beta^{3/2}, \qquad D_\beta = 1 - \frac{C_\beta(t_{\mathrm{hold}})}{C_{\beta,0}}, \tag{1}$$

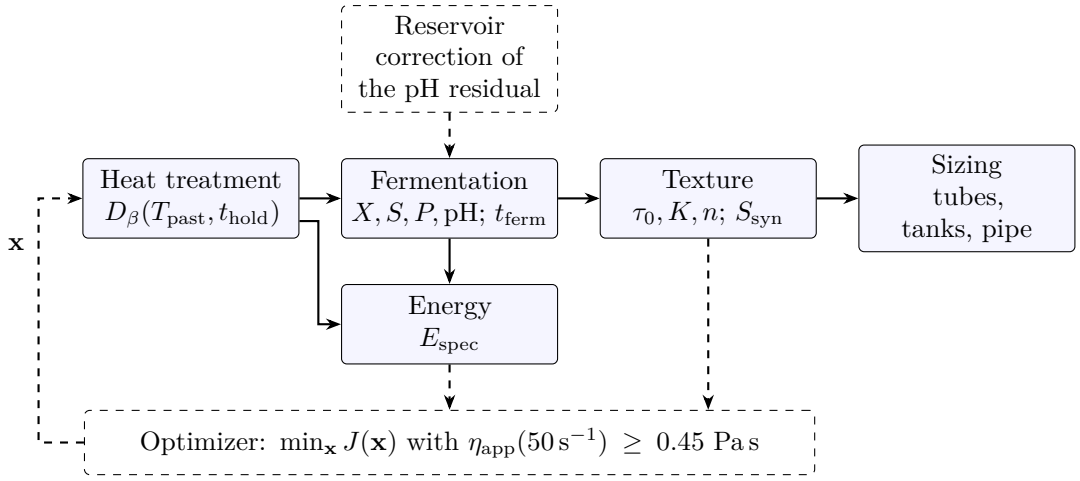

Figure 1: Structure of the model. Solid arrows carry state variables from one stage to the next; dashed elements are the data-driven correction and the optimization loop, which sets the operating variables $\mathbf{x}$. The degree of denaturation D_β is passed through to the texture stage; the heat treatment does not act on the fermentation kinetics; energy depends on the temperatures and the holding time, not on texture.

with $C_{\beta,0} = 3.2$ kg m^{-3}, close to the usual concentration of about 3.3 g/L in bovine milk [12]. The rate constant follows an Arrhenius law with a break at 90 °C, as found in [1]: below the break, $E_a = 265$ kJ mol^{-1}, within the range of 265–280 kJ mol^{-1} reported for skim and whole milk [1, 13]; above it, $E_a = 54$ kJ mol^{-1}, with k_d continuous at 363.15 K. The pre-exponential factor below the break is 6.02×10^{35} kg$^{-1/2}$ m$^{3/2}$ s^{-1}, which gives $k_d = 1.353 \times 10^{-3}$, 4.606×10^{-3} and 5.873×10^{-3} kg$^{-1/2}$ m$^{3/2}$ s^{-1} at 85, 90 and 95 °C. I could not trace this value back to the tables of [1]. It has to be checked against them, or refitted on plant measurements, before any quantitative use.

3.2 Fermentation and acidification

Biomass X, lactose S, lactic acid P and pH obey

$$\frac{\mathrm{d}X}{\mathrm{d}t} = (\mu - k_{\text{dec}})X, \qquad \mu = \mu_{\max}\,\gamma(T_{\text{ferm}})\,\frac{S}{K_S + S}\Big(1 - \frac{P}{P_{\max}}\Big)^{m_p}, \tag{2}$$

$$\frac{\mathrm{d}P}{\mathrm{d}t} = \alpha_{\text{LP}}\max\Big(0, \frac{\mathrm{d}X}{\mathrm{d}t}\Big) + \beta_{\text{LP}}X, \qquad \frac{\mathrm{d}S}{\mathrm{d}t} = -\frac{\mu X}{Y_{X/S}} - m_S X, \tag{3}$$

$$\frac{\mathrm{d}\,\text{pH}}{\mathrm{d}t} = -\frac{1}{M_{\text{LA}}\,\beta_{\text{buf}}(\text{pH})}\frac{\mathrm{d}P}{\mathrm{d}t}, \qquad \beta_{\text{buf}}(\text{pH}) = \beta_0 + \beta_{\text{CCP}}\exp\Big[-\frac{(\text{pH} - 5.15)^2}{2\sigma^2}\Big]. \tag{4}$$

The temperature factor γ is the cardinal temperature model with inflection of Rosso et al. [2],

$$\gamma(T) = \frac{(T - T_{\max})(T - T_{\min})^2}{(T_{\text{opt}} - T_{\min})\big[(T_{\text{opt}} - T_{\min})(T - T_{\text{opt}}) - (T_{\text{opt}} - T_{\max})(T_{\text{opt}} + T_{\min} - 2T)\big]} \tag{5}$$

for $T_{\min} < T < T_{\max}$ and 0 otherwise. Product formation follows Luedeking and Piret [3]. The buffer capacity of milk has a maximum near pH 5.1, which is associated with the dissolution of colloidal calcium phosphate [6]; the Gaussian term in (4) is only a convenient way to place that maximum and was not fitted. Table 2 lists the parameters. The initial state is $X_0 = 0.04$, $S_0 = 48$ and $P_0 = 0.15$ kg m^{-3} with $\text{pH}_0 = 6.65$; integration stops when the pH reaches 4.60, which defines t_{ferm}.

Table 2: Fermentation parameters (literature-based estimates, not fitted to the site).

Symbol	Value	Unit	Symbol	Value	Unit
$\mu_{\max}$	3.2×10^{-4}	s^{-1}	$Y_{X/S}$	0.14	$\mathrm{kg\ kg}^{-1}$
K_S	1.5	$\mathrm{kg\ m}^{-3}$	m_S	2.5×10^{-5}	$\mathrm{kg\ kg}^{-1}\ \mathrm{s}^{-1}$
$P_{\max}$	16	$\mathrm{kg\ m}^{-3}$	$T_{\min}, T_{\mathrm{opt}}, T_{\max}$	293.15, 315.15, 325.15	K
m_p	1.2	–	$\beta_0, \beta_{\mathrm{CCP}}$	22, 28	$\mathrm{mol\ m}^{-3}\ \mathrm{pH}^{-1}$
k_{dec}	1.2×10^{-5}	s^{-1}	σ	0.45	pH
α_{LP}	3.8	$\mathrm{kg\ kg}^{-1}$	M_{LA}	0.09008	$\mathrm{kg\ mol}^{-1}$
β_{LP}	8.5×10^{-5}	$\mathrm{kg\ kg}^{-1}\ \mathrm{s}^{-1}$			

3.3 Texture, syneresis and energy

Smoothing and pumping break part of the protein network. I describe what is left of it by the equilibrium of a rupture–recovery balance,

$$\lambda_{\mathrm{eq}} = \frac{k_{\mathrm{rec}}}{k_{\mathrm{rec}} + k_{\mathrm{rup}}\dot{\gamma}_{\mathrm{pump}}}, \qquad k_{\mathrm{rec}} = 0.015\ \mathrm{s}^{-1}, \quad k_{\mathrm{rup}} = 3.5 \times 10^{-4}, \tag{6}$$

and the stirred gel at 4 °C by the Herschel–Bulkley law [4],

$$\tau = \tau_0 + K\dot{\gamma}^{\,n}, \qquad \eta_{\mathrm{app}}(\dot{\gamma}) = \frac{\tau_0}{\dot{\gamma}} + K\dot{\gamma}^{\,n-1}, \qquad n = 0.42. \tag{7}$$

The yield stress and the consistency index increase with the degree of denaturation and with λ_{eq}, and decrease when fermentation stops away from pH 4.60:

$$K = (1.8 + 6.4 D_\beta^{1.3})(0.35 + 0.65\lambda_{\mathrm{eq}})\, e^{-8(\mathrm{pH_{stop}} - 4.6)^2} \quad [\mathrm{Pa\,s}^n], \tag{8}$$

$$\tau_0 = (2.5 + 14 D_\beta^{1.5})(0.25 + 0.75\lambda_{\mathrm{eq}})\, e^{-8(\mathrm{pH_{stop}} - 4.6)^2} \quad [\mathrm{Pa}]. \tag{9}$$

The mass fraction of whey expelled, used as a syneresis index, is

$$S_{\mathrm{syn}} = 0.28\,(1 - 0.72 D_\beta)(1.15 - 0.45\lambda_{\mathrm{eq}})\,[1 + 4.5(\mathrm{pH_{stop}} - 4.6)^2]. \tag{10}$$

Relations (8)–(10) only encode the direction of each effect: more denatured whey protein makes a firmer gel that holds its whey better, more shear makes a weaker one. I set their coefficients by hand so that the results fall in a plausible range, without any rheological or syneresis data. The quality constraint is $\eta_{\mathrm{app}}(50\ \mathrm{s}^{-1}) \geq 0.45$ Pa s.

The specific energy is the sum of three terms. Heating uses a regenerative exchanger of effectiveness $\eta_{\mathrm{rec}} = 0.85$, but the treated milk can give up its heat only down to the inoculation temperature T_{ferm}, so that

$$q_{\mathrm{heat}} = c_p\big[(T_{\mathrm{past}} - T_{\mathrm{raw}}) - \min\big(\eta_{\mathrm{rec}}(T_{\mathrm{past}} - T_{\mathrm{raw}}),\, T_{\mathrm{past}} - T_{\mathrm{ferm}}\big)\big], \tag{11}$$

with $c_p = 3930\ \mathrm{J\,kg}^{-1}\,\mathrm{K}^{-1}$ and $T_{\mathrm{raw}} = 4\,^\circ\mathrm{C}$. Without the cap, milk treated at 95 °C would leave the regeneration section at about 17.7 °C and would have to be heated again. Heat losses in the holding tube are $q_{\mathrm{hold}} = (U\,A/V)\,(T_{\mathrm{past}} - T_{\mathrm{amb}})\,t_{\mathrm{hold}}/\rho$, with $U = 1.2\ \mathrm{W\,m}^{-2}\,\mathrm{K}^{-1}$, $A/V = 4/D_{\mathrm{hold}}$, $D_{\mathrm{hold}} = 0.081$ m and $T_{\mathrm{amb}} = 25\,^\circ\mathrm{C}$, and cooling from T_{ferm} to 4 °C costs $q_{\mathrm{cold}} = c_p(T_{\mathrm{ferm}} - 277.15)/\mathrm{COP}$ with COP = 3.2. The sum $E_{\mathrm{spec}} = q_{\mathrm{heat}} + q_{\mathrm{hold}} + q_{\mathrm{cold}}$ thus mixes heat and electricity. That is good enough for comparing operating points, but it would be wrong in a primary-energy balance.

3.4 Data-driven correction of the pH residual

The mechanistic model leaves a residual $\boldsymbol{\delta}(t) = \mathbf{y}_{\text{plant}}(t) - \mathbf{y}_{\text{model}}(t)$ on the measured pH and lactic acid. I model it with an echo state network [5]: a fixed random recurrent reservoir of 80 units, density 0.15 and spectral radius 0.90, driven by standardized inputs $\mathbf{u}(t)$ (normalized time and the model values of pH, P and X),

$$\mathbf{r}(t) = \tanh\!\big(W\mathbf{r}(t-1) + W_{\text{in}}\mathbf{u}(t) + \mathbf{b}\big), \qquad \boldsymbol{\delta}(t) \approx W_{\text{out}} \begin{bmatrix} 1 \\ \mathbf{r}(t) \end{bmatrix}, \tag{12}$$

where only W_{out} is trained, by ridge regression with penalty 10^{-3} after a warm-up of 10 steps. (A spectral radius below one is the usual rule of thumb for the echo state property; it does not guarantee it.) The implementation uses ReservoirPy [10].

Because no plant data were available, the plant signal was generated from the model itself: the model trajectory at 42 °C (run to pH 4.50) was sampled at 240 points, and a drift and Gaussian noise were added,

$$\text{pH}_{\text{plant}} = \text{pH} + \Delta_{\text{pH}}(s) + 0.004\,\xi, \qquad P_{\text{plant}} = P + 0.22\,s^{1.3} + 0.015\,\xi', \qquad \Delta_{\text{pH}}(s) = -0.045\sin(2\pi s) + 0.03\,s^{1.5}, \tag{13}$$

with $s \in [0,1]$ the normalized time and ξ, ξ' standard normal variables. The network is trained on the first 70% of the batch (168 points) and evaluated on the last 30% (72 points). The result depends on the random reservoir, so I report it over 20 seeds.

3.5 Optimization

The objective combines fermentation time, syneresis and energy, each normalized by its value at the nominal point $\mathbf{x}_0 = (363.15\ \text{K}, 300\ \text{s}, 315.15\ \text{K}, 140\ \text{s}^{-1})$, plus a quadratic penalty on the viscosity constraint:

$$J(\mathbf{x}) = w_1 \frac{t_{\text{ferm}}}{t_{\text{ref}}} + w_2 \frac{S_{\text{syn}}}{S_{\text{ref}}} + w_3 \frac{E_{\text{spec}}}{E_{\text{ref}}} + 100\max\!\big(0,\ 0.45 - \eta_{\text{app}}(50\ \text{s}^{-1})\big)^2, \tag{14}$$

with $(w_1, w_2, w_3) = (0.4, 0.4, 0.2)$ unless stated otherwise. The bounds are $T_{\text{past}} \in [85, 95]$ °C, $t_{\text{hold}} \in [180, 600]$ s, $T_{\text{ferm}} \in [38, 45]$ °C and $\dot\gamma_{\text{pump}} \in [60, 250]$ s^{-1}. The minimization uses the bounded Nelder–Mead method of SciPy [11].

3.6 Equipment sizing

For a mass flow $\dot m = 2.5$ kg s^{-1} ($\rho = 1030$ kg m^{-3}, $\dot V = 2.427 \times 10^{-3}$ m^3 s^{-1}), the holding tube has volume $\dot V t_{\text{hold}}$; with a DN80 hygienic tube (85 × 2 mm, inner diameter 0.081 m) its length follows directly. Fermentation takes place in $N = 4$ tanks used in rotation under continuous feed. Each tank is occupied during filling, fermentation and $t_{\text{CIP}} = 5400$ s of emptying and cleaning, and rotation requires $N t_{\text{fill}} = t_{\text{fill}} + t_{\text{ferm}} + t_{\text{CIP}}$, so that, with a filling ratio $\phi = 0.82$ and $H/D = 1.6$,

$$V_{\text{tank}} = \frac{\dot V (t_{\text{ferm}} + t_{\text{CIP}})}{(N-1)\,\phi}. \tag{15}$$

The transfer pipe after fermentation is sized so that the wall shear rate equals $\dot\gamma_{\text{pump}}$. For a power-law fluid of index n the Rabinowitsch–Mooney relation [8, 9] gives

$$D_{\text{pipe}} = \Big(\frac{3n+1}{4n}\,\frac{32\dot V}{\pi \dot\gamma_{\text{pump}}}\Big)^{1/3}, \qquad \frac{\Delta P}{L} = \frac{4\tau_w}{D_{\text{pipe}}}, \quad \tau_w = \tau_0 + K\dot\gamma_{\text{pump}}^{\,n}. \tag{16}$$

This ignores the yield stress in the flow rate, so I also compute the diameter for the full Herschel–Bulkley law, from $\dot V = (\pi R^3/\tau_w^3)\int_{\tau_0}^{\tau_w} \tau^2\big((\tau-\tau_0)/K\big)^{1/n}\,\mathrm{d}\tau$. The flow regime is checked with the Metzner–Reed Reynolds number [7], both in its power-law form and in the generalized form $\text{Re} = 8\rho v^2/\tau_w$, which includes τ_0.

4 Implementation

The model is a Python notebook (NumPy, SciPy [11], ReservoirPy 0.4.3 [10], Matplotlib). The ordinary differential equations are integrated with the explicit Runge–Kutta method DOP853 (relative tolerance 10^{-9} for denaturation and 10^{-8} for fermentation), with event detection to stop fermentation at the target pH. The notebook also contains an interactive simulator, a three-dimensional schematic of the line with STL export, and a NumPy implementation of the echo state network used when ReservoirPy is not installed; none of them is used for the results below. All numbers below were obtained by rerunning the notebook from scratch with Python 3.13, NumPy 2.5.3 and SciPy 1.18.1; they agree with the values stored in the notebook, which were produced with earlier versions of NumPy and SciPy. The additional analyses (multi-start optimization, sensitivity to the weights, exact Herschel–Bulkley diameter) and the figures are produced by two short scripts provided with the notebook.

5 Results

5.1 Heat treatment and fermentation

For a holding time of 300 s, the model gives $D_\beta = 0.462$, 0.800 and 0.849 at 85, 90 and 95 °C. Most of the gain occurs below 90 °C, where the activation energy is high; above the break, the rate grows slowly with temperature, and longer holding becomes the more effective way to increase D_β (Figure 2(a)).

At 42 °C the pH reaches 4.60 after $t_{\mathrm{ferm}} = 14\,726$ s (4.09 h), with final biomass 1.61 kg m^{-3} and lactic acid 6.74 kg m^{-3} (Figure 2(b,c)). The fermentation time has a flat minimum at 42 °C, the optimal temperature of the cardinal model: it stays between 4.09 and 4.12 h from 41 to 43 °C, and rises to 4.53 h at 38 °C and 4.72 h at 46 °C (Figure 2(d)). In this model the heat treatment does not affect fermentation; it acts only on texture and energy.

5.2 Correction of the residual on synthetic data

On the validation window, where the model pH falls from 5.52 to 4.50, the mechanistic model alone has a root-mean-square error of 0.0558 pH unit with respect to the synthetic plant signal. With the echo state network the median error over 20 seeds is 0.0256, a reduction of 54%, with a range of 0.0048 to 0.0539; the corrected model is better than the model alone for all 20 seeds (Figure 3). The seed shown in Figure 3(a) is the one closest to the median (0.0221). So the network can learn a smooth drift of this kind from the first 70% of a batch and carry it to the end. How large the residual would be on a real line is a separate question that these runs cannot answer.

5.3 Optimal operating point

Table 3 compares the nominal and optimal points. The optimizer converged after 107 evaluations to $T_{\mathrm{past}} = 95$ °C, $t_{\mathrm{hold}} = 600$ s, $T_{\mathrm{ferm}} = 41.05$ °C and $\dot\gamma_{\mathrm{pump}} = 60$ s^{-1}: three of the four variables are at a bound. Ten runs, one from the nominal point and nine from random starting points, all ended at the same point, with $J = 0.879$ against 1.000 at the nominal point. The nominal point itself violates the viscosity constraint very slightly (0.449 against 0.45 Pa s).

The corner solution is easy to explain. Syneresis decreases with D_β and with λ_{eq} (Figure 4(b)), so it pushes T_{past} and t_{hold} up and $\dot\gamma_{\mathrm{pump}}$ down, and nothing in J pushes back. In particular, once the cap in (11) is active, the heating duty equals $c_p(T_{\mathrm{ferm}} - T_{\mathrm{raw}})$ and no longer depends on T_{past}. Table 4 shows the energy terms: heating accounts for about 75% of E_{spec}, and the small reduction at the optimum comes from the lower fermentation temperature, which reduces both heating and cooling, partly offset by larger losses in the longer holding tube. Only T_{ferm} is set by

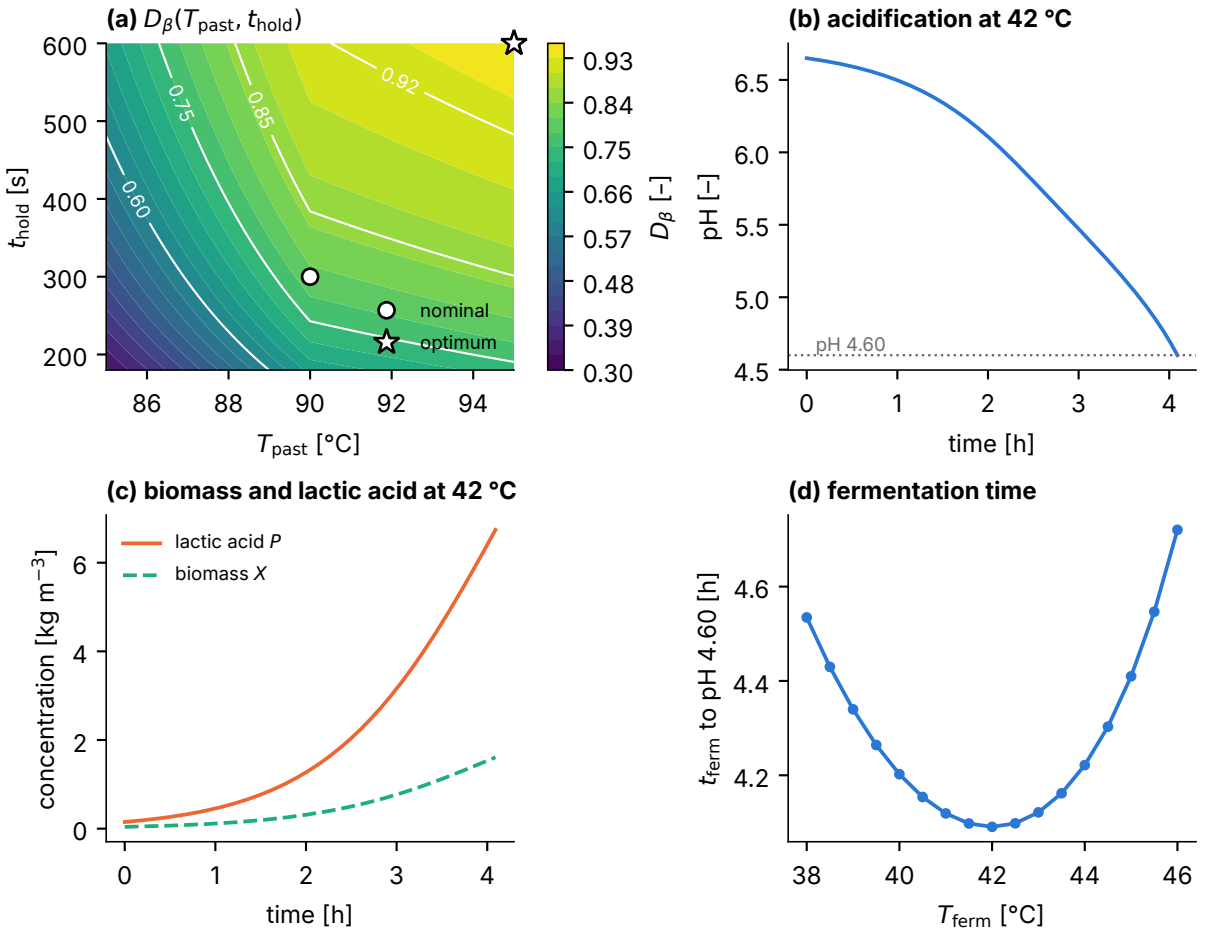

Figure 2: (a) Degree of denaturation of β-lactoglobulin as a function of heat-treatment temperature and holding time; the kink of the contours at 90 °C comes from the break in the Arrhenius law. (b, c) pH, lactic acid and biomass during fermentation at 42 °C. (d) Time to reach pH 4.60 as a function of fermentation temperature.

a genuine trade-off, between fermentation time, which favours 42 °C, and energy, which favours lower temperatures.

Changing the weights gives the same picture (Table 5). As long as syneresis has a positive weight, the optimum keeps T_{past}, t_{hold} and $\dot{\gamma}_{pump}$ at their bounds, and the weights only move T_{ferm}, from 41.4 °C when fermentation time dominates to the lower bound of 38 °C when energy dominates. When only energy counts, the heat treatment is relaxed until the viscosity constraint becomes active (0.450 Pa s); when only fermentation time counts, the optimizer stays near the nominal point, since nothing else matters. For the optimization to say something useful, J would need terms for fouling of the heating section, cooked flavour and the cost of the holding tube, which would stop the heat treatment before the bounds.

5.4 Sensitivity to the climate of the site

At the optimal point, using the annual mean temperature of Akbou (17.6 °C) as the hall temperature changes E_{spec} by only +0.13%, through the losses of the holding tube. Using the mean July maximum (34 °C) together with a lower coefficient of performance of the refrigeration plant in summer (COP = 2.6 instead of 3.2) raises it by 5.3%, to 203.7 kJ kg^{-1}. Almost all of the increase comes from the COP value, which I guessed; the manufacturer's curve for the actual units should replace it.

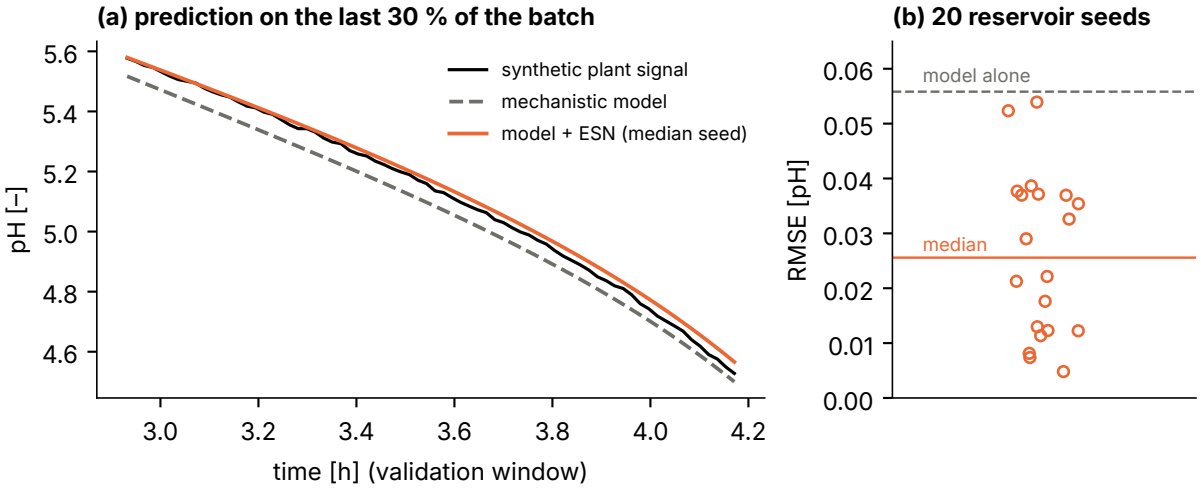

Figure 3: Hybrid model on synthetic plant data. (a) pH on the validation window: synthetic plant signal, mechanistic model, and model corrected by the echo state network for the seed closest to the median error. (b) Error of the corrected model for 20 reservoir seeds, compared with the error of the model alone.

Table 3: Nominal and optimal operating points, weights $(0.4, 0.4, 0.2)$.

Quantity	Nominal	Optimum	Change
T_{past} [°C]	90.00	95.00	+5.00 K
t_{hold} [s]	300	600	+100%
T_{ferm} [°C]	42.00	41.05	−0.95 K
$\dot{\gamma}_{\mathrm{pump}}$ [s^{-1}]	140	60	−57%
D_β [–]	0.800	0.942	+17.8%
t_{ferm} [h]	4.09	4.12	+0.6%
τ_0 [Pa]	5.33	8.61	+61%
$\eta_{\mathrm{app}}(50\ \mathrm{s}^{-1})$ [Pa s]	0.449	0.668	+49%
S_{syn} [%]	12.40	8.67	−30%
E_{spec} [kJ kg^{-1}]	197.1	193.5	−1.8%

5.5 Equipment sizing

Table 6 gives the dimensions at the optimal point. The holding tube needed for 600 s in DN80 is 283 m long (141 m for the nominal 300 s); a line of this length is unusual, and a holding cell of larger diameter or a holding tank would normally be preferred. The transfer pipe is 82.2 mm in diameter when the yield stress is neglected and 86.8 mm with the full Herschel–Bulkley law, a difference of about 5%; the flow is laminar by a wide margin in both cases.

6 Discussion and limitations

The model is easy to follow and to modify, and it makes a few familiar design facts explicit: above 90 °C temperature does little for denaturation, the fermentation optimum is flat, heating dominates the energy bill, and long holding times mean very long tubes. Its numbers, on the other hand, should not be read as statements about a real plant.

The kinetic parameters are literature estimates for standardized bovine milk, the pre-exponential factor of the denaturation law is unverified, and the texture and syneresis laws (8)–(10) are not fitted. Each stage is treated as perfectly mixed, which may not hold in tanks of 20 m^3; as a working rule I would take a measured axial temperature difference above about 0.5 K as a

Table 4: Terms of the specific energy [kJ kg^{-1}].

	q_{heat}	q_{hold}	q_{cold}	E_{spec}
Nominal	149.3	1.1	46.7	197.1
Optimum	145.6	2.4	45.5	193.5

Table 5: Optimum as a function of the weights (w_1, w_2, w_3) in (14), started from the nominal point.

(w_1, w_2, w_3)	T_{past} [°C]	t_{hold} [s]	T_{ferm} [°C]	$\dot{\gamma}_{\mathrm{pump}}$ [s^{-1}]	t_{ferm} [h]	S_{syn} [%]	E_{spec} [kJ/kg]
$(0.4, 0.4, 0.2)$	95.0	600	41.05	60	4.12	8.67	193.5
$(0.6, 0.2, 0.2)$	95.0	600	41.37	60	4.10	8.67	195.2
$(0.2, 0.6, 0.2)$	95.0	600	40.06	60	4.20	8.67	188.4
$(0.2, 0.2, 0.6)$	95.0	600	38.00	60	4.53	8.67	177.8
$(0, 0, 1)$	89.5	180	38.00	60	4.53	14.66	176.0
$(1, 0, 0)$	90.1	315	42.00	140	4.09	12.15	197.2

sign that a spatially resolved model is needed, though no standard backs that threshold. The correction was trained on signals produced by the model itself. The optimum sits at the bounds because fouling, flavour and capital cost are missing from (14), and the energy indicator mixes heat and electricity. Finally, singular pressure losses in bends, valves and fittings are ignored, and the power-law sizing underestimates the pipe diameter by about 5%.

Calibrating the model on a real line would take four sets of measurements. Native β-lactoglobulin at the outlet of the holding section, by reversed-phase HPLC or ELISA, for several temperature and time settings, would identify the denaturation law. pH and temperature records from 20 to 30 batches spread over both collection seasons, with the share of reconstituted milk of each batch recorded as an input of the correction, would give the residual something real to learn. Flow curves between 0.1 and 300 s^{-1} at 4 °C and syneresis by centrifugation would replace (8)–(10) by fitted relations. Hall temperature and the actual COP of the refrigeration units in summer would settle the climate effect. The optimization should then be run again with penalties for fouling and capital cost.

7 Conclusion

The coupled model runs from heat treatment to equipment size and keeps track of which of its parts are established and which are assumed. With literature parameters it gives the expected orders of magnitude. Its optimization mainly shows what the objective lacks: as long as fouling, flavour and capital cost are left out, the heat treatment will be pushed to its upper bounds. Using it for a given plant requires the measurements listed in Section 6.

Data and code availability

The notebook that implements the model, together with the scripts that produce the additional analyses and the figures, is provided as ancillary files with this preprint. All plant-related figures come from the public sources cited; no company data were used.

Conflict of interest

The author has no affiliation with, and received no information or funding from, the company whose site is used as a case study.

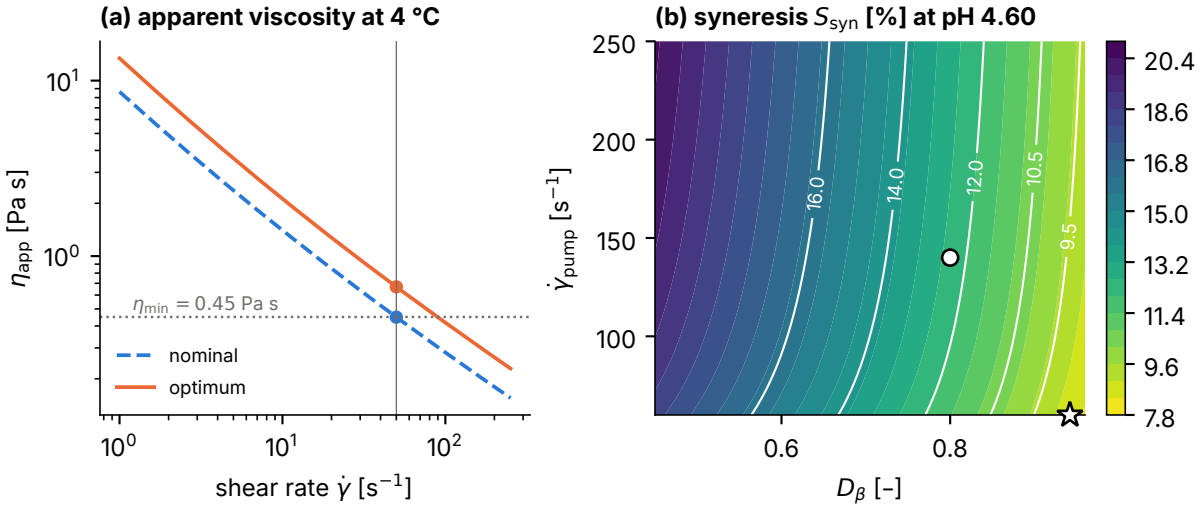

Figure 4: (a) Apparent viscosity of the stirred gel at 4 °C at the nominal and optimal points; the dots mark the quality criterion at 50 s^{-1}. (b) Syneresis index as a function of the degree of denaturation and of the smoothing shear, for fermentation stopped at pH 4.60; circle: nominal point, star: optimum.

Table 6: Equipment dimensions at the optimal point, $\dot{m} = 2.5$ kg s^{-1}.

Equipment	Quantity	Value
Holding tube (DN80)	volume, length, mean velocity	1.456 m^3, 282.6 m, 0.471 m s^{-1}
Fermentation tanks ($N = 4$)	volume, diameter, height	19.95 m^3, 2.51 m, 4.02 m
	filling time	1.87 h
Transfer pipe	inner diameter, power law / Herschel–Bulkley	82.15 mm / 86.83 mm
	mean velocity (power-law diameter)	0.458 m s^{-1}
	wall stress, pressure gradient	35.4 Pa, 1722 Pa m^{-1}
	Reynolds number, power law / generalized	64.6 / 48.9

References

[1] F. Dannenberg, H. G. Kessler, Reaction kinetics of the denaturation of whey proteins in milk, *J. Food Sci.* 53(1) (1988) 258–263.

[2] L. Rosso, J. R. Lobry, J. P. Flandrois, An unexpected correlation between cardinal temperatures of microbial growth highlighted by a new model, *J. Theor. Biol.* 162 (1993) 447–463.

[3] R. Luedeking, E. L. Piret, A kinetic study of the lactic acid fermentation. Batch process at controlled pH, *J. Biochem. Microbiol. Technol. Eng.* 1 (1959) 393–412.

[4] W. H. Herschel, R. Bulkley, Konsistenzmessungen von Gummi-Benzollösungen, *Kolloid-Z.* 39 (1926) 291–300.

[5] H. Jaeger, The “echo state” approach to analysing and training recurrent neural networks, GMD Report 148, German National Research Center for Information Technology, 2001.

[6] J. A. Lucey, P. F. Fox, Importance of calcium and phosphate in cheese manufacture: a review, *J. Dairy Sci.* 76 (1993) 1714–1724.

[7] A. B. Metzner, J. C. Reed, Flow of non-Newtonian fluids—correlation of the laminar, transition, and turbulent-flow regions, *AIChE J.* 1 (1955) 434–440.

[8] B. Rabinowitsch, Über die Viskosität und Elastizität von Solen, *Z. Phys. Chem. A* 145 (1929) 1–26.

[9] M. Mooney, Explicit formulas for slip and fluidity, *J. Rheol.* 2(2) (1931) 210–222.

[10] N. Trouvain, L. Pedrelli, T. T. Dinh, X. Hinaut, ReservoirPy: an efficient and user-friendly library to design echo state networks, in: *Artificial Neural Networks and Machine Learning – ICANN 2020*, Springer, 2020, pp. 494–505.

[11] P. Virtanen et al., SciPy 1.0: fundamental algorithms for scientific computing in Python, *Nat. Methods* 17 (2020) 261–272.

[12] G. Konrad, B. Lieske, W. Faber, A large-scale isolation of native β-lactoglobulin: characterization of physicochemical properties and comparison with other methods, *Int. Dairy J.* 10(10) (2000) 713.

[13] S. G. Anema, A. B. McKenna, Reaction kinetics of thermal denaturation of whey proteins in heated reconstituted whole milk, *J. Agric. Food Chem.* 44 (1996) 422.

[14] TSA, "Bataille de l'or blanc : le modèle original de Soummam", https://www.tsa-algerie.com/?p=259912 (accessed November 2026).

[15] Algérie-Éco, "Laiterie Soummam : 250 millions de litres de lait collectés en 2024", https://algerie-eco.com/?p=212874 (accessed November 2026).

[16] TSA, "La Laiterie Soummam revendique la plus grande ferme laitière d'Algérie", https://www.tsa-algerie.com/la-laiterie-soummam-revendique-la-plus-grande-ferme-laitiere-dalgerie/ (accessed November 2026).

[17] TSA, "Collecte de lait cru : les révélations du patron de Soummam", https://www.tsa-algerie.com/collecte-de-lait-cru-les-revelations-du-patron-de-soummam/ (accessed November 2026).

[18] Algérie-Éco, "Laiterie Soummam : réalisation d'une station d'épuration des eaux usées", https://algerie-eco.com/?p=173111 (accessed November 2026).

[19] Open Food Facts, product 6130760001529, "Brassé aromatisé – Soummam – 90 g", https://world.openfoodfacts.org/product/6130760001529 (accessed November 2026).

[20] wfy24, "Climate data Akbou", https://www.wfy24.com/en/climate/akbou-dz418104397 (accessed November 2026).